

Neural Fractional Differential Equations

C. Coelho^{1*}, M. Fernanda P. Costa¹ and L.L. Ferrás^{1,2}

¹Centre of Mathematics (CMAT), University of Minho, Braga, 4710-57, Portugal.

²Department of Mechanical Engineering (Section of Mathematics) - FEUP, University of Porto, Porto, 4200-465, Portugal.

*Corresponding author(s). E-mail(s): cmartins@cmat.uminho.pt;
Contributing authors: mfc@math.uminho.pt; lferras@fe.up.pt;

Abstract

Fractional Differential Equations (FDEs) are essential tools for modelling complex systems in science and engineering. They extend the traditional concepts of differentiation and integration to non-integer orders, enabling a more precise representation of processes characterised by non-local and memory-dependent behaviours. This property is useful in systems where variables do not respond to changes instantaneously, but instead exhibit a strong memory of past interactions. Having this in mind, and drawing inspiration from Neural Ordinary Differential Equations (Neural ODEs), we propose the Neural FDE, a novel deep neural network architecture that adjusts a FDE to the dynamics of data. This work provides a comprehensive overview of the numerical method employed in Neural FDEs and the Neural FDE architecture. The numerical outcomes suggest that, despite being more computationally demanding, the Neural FDE may outperform the Neural ODE in modelling systems with memory or dependencies on past states, and it can effectively be applied to learn more intricate dynamical systems.

Keywords: Neural Fractional Differential Equations, Neural Ordinary Differential Equations, Neural Networks, Time-Series, Numerical Methods.

1 Introduction

Real systems in science and engineering, exhibit complex behaviours, often characterised by intricate dynamics, non-linear interactions, and emergent phenomena. These

complexities arise in various contexts, such as the complex interactions of molecules within a cell, the chaotic movement of turbulent flows, and the challenging task of predicting financial markets.

To effectively predict and understand these complex systems, mathematical models are employed, allowing to gain insights into the system behaviour without the need for time-consuming or expensive experiments.

Due to the inherent presence of continuous dynamics in these systems, Differential Equations (DEs) are commonly employed as mathematical models, accounting for the continuous evolution of the system's behaviour and offering the advantage of enabling predictions throughout the entire time domain and not only at specific points.

With the emergence of Neural Networks (NNs) and their impressive performance in fitting mathematical models to data, numerous studies have focused on modelling real-world systems. However, conventional NNs are designed to model discrete functions and may not be able to accurately capture the continuous dynamics observed in several systems. To overcome this limitation, Chen et al. [1] introduced the Neural Ordinary Differential Equations (Neural ODEs), a NN architecture that adjusts an Ordinary Differential Equation (ODE) to the dynamics of a system.

ODEs are favored for their simplicity and effectiveness in describing the instantaneous rates of change within a system. However, they may not adequately model systems with more complex memory or strong dependence on past states beyond the immediate previous states. To address this issue, Fractional Differential Equations (FDEs) have been introduced [2]. FDEs expand the notion of derivatives to fractional orders, facilitating the modelling of systems with memory or non-local interactions. They use all past states to predict the current and future behaviours of the system and capture fractional-order rates of variable changes, offering a more thorough representation of the system dynamics. Consequently, FDEs enable an accurate depiction of systems with memory or long-range dependencies [3].

Inspired by Neural ODEs and by the inherent memory of FDEs, in a preliminary work, we briefly proposed a novel deep learning architecture that models a FDE to the hidden dynamics of the data [4]. To the best of our knowledge, this is the first time that a NN architecture is proposed to fully fit a FDE to the dynamics of data, including the order of the fractional derivative. In this paper, we build upon our prior work [4] by introducing several new and significant contributions:

- **Background:** we incorporate a concise background section, providing essential context to comprehending and understanding the proposed Neural FDE, namely on Neural ODEs and FDEs;
- **Justification:** we add a detailed explanation of the mechanisms underlying Neural FDEs and their theoretical advantages, thereby establishing a robust justification for their adoption;
- **Computational cost:** we conduct a thorough analysis of the time and memory complexity of Neural FDEs, providing insights into the computational efficiency of our proposed method;
- **Numerical experiments:** we augment the numerical experiments in [4] by introducing three additional systems from various fields: relaxation oscillation process, resistor-capacitor circuit, and a substance decay process. For each system, we include

datasets obtained from the solution of FDEs considering different orders of the derivative (α) totalling five α values and one ODE ($\alpha = 1$). Additionally, we investigate the model’s robustness and generalisation by testing with higher-frequency sampling and for larger time interval sets;

- Learnt derivative order analysis: we explore the learnt values of α (the order of the fractional derivate) to discern potential patterns in the learning process;
- Convergence analysis: we conduct a series of experiments and analysis to assess the convergence properties and stability of Neural FDEs, providing valuable insights into the reliability of our proposed method;
- Developed datasets: we meticulously present and describe the datasets used in our numerical experiments for the four systems, elucidating the processes behind their generation.

This paper is organised as follows. Section 2 presents a brief review of essential concepts such as FDEs and Neural ODEs. Section 3 presents the Neural FDE architecture along with its mathematical formulation and algorithm. In Section 4 we evaluate the performance of the newly proposed Neural FDE. We use datasets describing two real-world systems to compare the performance of Neural FDE with a Neural ODE baseline. The paper ends with the summary of the findings and future directions in Section 5. Additionally, in Appendix A we provide an explanation on the impact of refining meshes and in Appendix B we present numerical results for two additional real-world system datasets.

2 Background

Consider a time series, denoted as $\mathbf{X} = (\mathbf{x}_0, \mathbf{x}_1, \dots, \mathbf{x}_{N-1})$, where each element $\mathbf{x}_n \in \mathbb{R}^d$ represents the state of the system at instant t_n ($n = 0, \dots, N - 1$). Similarly, let $\mathbf{Y} = (\mathbf{y}_1, \mathbf{y}_2, \dots, \mathbf{y}_{N^*})$ denote the associated ground-truth output time series. In this context, $\mathbf{y}_n \in \mathbb{R}^{d^*}$ is the output at time step t_n . Additionally, the predicted output time series is expressed as $\hat{\mathbf{Y}} = (\hat{\mathbf{y}}_1, \hat{\mathbf{y}}_2, \dots, \hat{\mathbf{y}}_{N^*})$, where each prediction $\hat{\mathbf{y}}_n \in \mathbb{R}^{d^*}$ corresponds to time step t_n . Note that N^* may differ from N .

Neural Ordinary Differential Equations

Residual Networks can be seen as a sequence of transformations to a hidden state, [5–10]. This sequence of transformations was originally proposed to be of the form (for a network with M layers):

$$\mathbf{h}_{j+1} = \mathbf{h}_j + F(\mathbf{h}_j, \boldsymbol{\theta}_j), \quad j = 0, \dots, M - 1 \quad (1)$$

with F being a function that depends on the state \mathbf{h}_j and on $\boldsymbol{\theta}_j$ (where $\boldsymbol{\theta}_j$ represents all the parameters of the network determined by the learning process [6] - the weight matrix and bias).

The *new* state, \mathbf{h}_{j+1} , is obtained by adding $F(\mathbf{h}_j, \boldsymbol{\theta}_j)$ to the *old* state, \mathbf{h}_j , and, for the residual forward problem presented in (1) to be stable, it is recommended to control the variation of $F(\mathbf{h}_j, \boldsymbol{\theta}_j)$ along the iterations. Therefore, in [6, 7] (see also [9]), the authors proposed an improved version of (1) (see (2)) by introducing a constant

δ — a positive constant enabling control over the variation of F (the smaller the δ the more control we have over the variation of F). This enhancement results in the following refined residual network:

$$\mathbf{h}_{j+1} = \mathbf{h}_j + \delta F(\mathbf{h}_j, \boldsymbol{\theta}_j), \quad j = 0, \dots, M - 1. \quad (2)$$

This equation can be rewritten as,

$$\frac{\mathbf{h}_{j+1} - \mathbf{h}_j}{\delta} = F(\mathbf{h}_j, \boldsymbol{\theta}_j), \quad j = 0, \dots, M - 1, \quad (3)$$

which is the explicit Euler discretization (with time-step δ) of the nonlinear ODE,

$$\frac{d\mathbf{h}(t)}{dt} = F(\mathbf{h}(t), \boldsymbol{\theta}(t)) \quad (4)$$

over the time interval $[0, T]$ (t is the time). The continuous nature of this problem is encapsulated in (4), which extends beyond the scope of (2). It introduces the capability to derive the solution or state for any given moment within the specified time interval. Several researchers have undertaken analytical studies on this continuous residual equation (4), which has also been extended to address more intricate differential equations (dynamical systems), as exemplified in [10].

Remark 1: To go from (3) to (4), one should have the property that as δ becomes smaller, the difference between \mathbf{h}_{j+1} and \mathbf{h}_j should also become smaller. This is in fact true, because in the limiting case of $\delta = 0$, we have from (2) that $\mathbf{h}_{j+1} = \mathbf{h}_j$.

Remark 2: While it is indeed true that the parameter δ provides a means to regulate the stability of the forward problem (2), the issue of stability is, in fact, a more intricate matter. It is not solely determined by δ but also influenced by the variations in the weight matrix – refer to [6, 7] for a comprehensive explanation.

In 2018, the Neural ODE framework was introduced [1]. Building upon (4), the authors [1] introduced a neural network (NN) architecture specifically tailored for modeling time-series data characterized by continuous-time dynamics. Unlike conventional NNs, which are confined to representing discrete dynamics, the use of Neural ODEs involves adjusting or fine-tuning a function (\mathbf{f}_θ) to ensure that the solution of the Initial Value Problem (IVP),

$$\frac{d\mathbf{h}(t)}{dt} = \mathbf{f}_\theta(\mathbf{h}(t), t) \quad \text{with} \quad \mathbf{h}(t_0) = \mathbf{h}_0, \quad (5)$$

accurately represents a dynamic system. Here, \mathbf{f}_θ represents the right-hand side of the ODE, given by a NN with parameters $\boldsymbol{\theta}$, where t denotes time, and $\mathbf{h}(t_0) = \mathbf{h}_0$ is the initial condition of the IVP, essentially capturing the state at the first instance of the provided data. This fine-tuning of \mathbf{f}_θ allows the solution of (5) to effectively fit the given data, capturing the behaviour of the dynamic system. The innovation in the Neural ODE, as compared to (4), lies in the calculation of $F(\mathbf{h}(t), \boldsymbol{\theta}(t))$ using a NN, $\mathbf{f}_\theta(\mathbf{h}(t), t)$, instead of using an analytical procedure.

In addition to the NN, the Neural ODEs are made up of a numerical ODE solver (referred to as *ODESolve*) for the numerical solution of the differential equation, and each state is then given by,

$$\{\mathbf{h}(t)\}_{t=t_0, t_1, \dots, t_f} = \text{ODESolve}(\mathbf{f}_\theta, \mathbf{h}_0, (t_0, t_1, \dots, t_f)),$$

where $\mathbf{h}(t)$ is the vector solution at instant t being t in the time interval $[t_0, t_f]$. With analogy to the discrete case, $\mathbf{h}(t_0)$ is the input layer and $\mathbf{h}(t_f)$ is the output layer. Since $t \in [t_0, t_f]$, for all values $t^* \in]t_0, t_f[$ we obtain $\mathbf{h}(t^*)$ that can be seen as a continuous version of hidden layers.

Remark 3: For simplicity we consider that the output of the numerical method is the output of the Neural ODE, $\hat{\mathbf{Y}}(\theta)$. However this may not be always the case and a second NN might be used to transform the solution of the numerical method into the prediction $\hat{\mathbf{Y}}(\theta)$.

The solver makes use of the \mathbf{f}_θ function, which takes the current state of the system \mathbf{h}_t as input, delivers the derivative of the state as output ($d\mathbf{h}(t)/dt$) and then integrates the derivative over time to determine the next state \mathbf{h}_{t+1} , that is:

$$\mathbf{h}_{t+1} = \mathbf{h}_t + \int_t^{t+1} \mathbf{f}_\theta(\mathbf{h}(t), t) dt.$$

The Neural ODE [1] allows the use of both adaptive and fixed-step solvers. When employing a fixed-step solver without explicitly specifying the step size Δt (default case), the time interval discretization occurs solely based on the time-steps forced by the time-series training data. However, when the step size is explicitly specified, the discretization takes place for each sub-interval (t_n, t_{n+1}) with the specified step size yielding $(t_{n+1} - t_n)/\Delta t$ time steps for each sub-interval. On the other hand, when using an adaptive-step solver, the discretization also occurs for each sub-interval (t_n, t_{n+1}) , but the step size is not predetermined, instead it is dynamically adjusted based on the local solution behaviour (local gradient) [11]. The refinement of the mesh inside each sub-interval allows for the solver to compute the solution with higher accuracy at an increased computational cost, for a detailed explanation on the implications of the use of different step sizes see Appendix A.

Fractional Differential Equations

FDEs are a class of differential equations that extend the concept of integer-order derivatives to non-integer (or fractional) orders. There exist different definitions for fractional derivatives, but for the purpose of this study, our exclusive focus will be on the Caputo fractional derivative of order α . It is denoted as ${}^C_0D_t^\alpha g(t)$ [12] (also refer to [2]), and can be expressed for a general function $g(t)$ as follows:

$${}^C_0D_t^\alpha g(t) = \frac{1}{\Gamma([\alpha] - \alpha)} \int_0^t (t - s)^{[\alpha] - \alpha - 1} g^{([\alpha])}(s) ds,$$

where α represents the order of the fractional derivative; the symbol $[\alpha]$ denotes the ceiling function applied to α (producing the smallest integer greater than or equal to α). Additionally, we make use of the Gamma function, denoted by Γ [2, 12, 13]. We

opt for this specific fractional derivative as it is more suited for modelling physical processes, since the initial conditions are based on integer-order derivatives.

In this study, we extend (4) by incorporating the Caputo fractional derivative (insights into the application of fractional calculus in Neural systems are discussed in [14], providing a rationale for this modification). This enhancement allows our dynamic system to encompass fractional rates and memory, and the resulting outcome is:

$${}_0^C D_t^\alpha \mathbf{h}(t) = \mathbf{f}(\mathbf{h}(t), t), \quad t > 0, \quad \mathbf{h}^{(k)}(t_0) = \mathbf{h}_0^k, \quad k = 0, \dots, \lceil \alpha \rceil - 1, \quad (6)$$

with (k) the derivative of integer-order k and $\mathbf{h}^{(k)}(t_0) = \mathbf{h}_0^k$ the k^{th} initial condition of the IVP (\mathbf{h}_0^k is the real value or the vector of real values associated with the k^{th} initial condition). Note that $\mathbf{f}(\mathbf{h}(t), t)$ represents a function and not a NN. If this function is continuous and fulfils a Lipschitz condition with respect to its first argument with Lipschitz constant L on a suitable set G then this equation has a unique solution on some interval $[0, T]$ [15].

Unlike integer-order derivatives found in ODEs, where the derivative's value at a point is solely dependent on the function's behaviour within an infinitesimal neighbourhood around that point (given an initial value, the solution is uniquely determined for any point of the domain [16]), fractional derivatives, as described by Equation (6), exhibit non-local characteristics. To compute the state \mathbf{h}_t , it is necessary to take into account the complete history from the initial state up to the current time, t , [13]:

$$\mathbf{h}_t = \sum_{k=0}^{\lceil \alpha \rceil - 1} \frac{t^k}{k!} \mathbf{h}_0^k + \frac{1}{\Gamma(\alpha)} \int_0^t (t-s)^{\alpha-1} \mathbf{f}(\mathbf{h}(s), s) ds.$$

While the non-locality of FDEs adds complexity and computational expense to their solution, this characteristic also means that FDEs inherently encompass memory effects [17]. This property proves beneficial in systems where variables don't respond instantaneously to changes but rather exhibit a memory of past interactions [3].

Remark 4: It's worth noting that FDEs have been previously proposed for analytical modelling of NNs, addressing aspects such as stability, bifurcations, and chaos (refer to [18] and the references therein). It's important to clarify that the objective of this work is not the analytical examination of (6), but rather the development of a Neural FDE.

3 Neural Fractional Differential Equations

Having in mind the concepts of Neural ODE [1] and fractional calculus in Neural systems [14], in [4] we introduced the Neural FDE, a NN architecture parameterised by θ (weights and biases) that adjusts the function \mathbf{f}_θ of a FDE of order α (see (7)). The goal is to ensure that the curve of solutions of this FDE fits the provided data accurately by changing the weights and biases in \mathbf{f}_θ .

Since this model has an extra parameter (α) when compared to the Neural ODE, the order of the FDE, α , is also learnt by another NN, α_ϕ , with parameters ϕ . This makes the process of adjusting (7) to the training data completely independent of any user intervention and gives the Neural FDE the freedom to find the best possible fit:

$${}^C_0D_t^\alpha \mathbf{h}(t) = \mathbf{f}_\theta(\mathbf{h}(t), t) \text{ with } \mathbf{h}(t_0) = \mathbf{h}_0, \quad \alpha = \alpha_\phi. \quad (7)$$

Remark 5: In this work we consider $\alpha \in (0, 1)$ since this is the case in many applications and simplifies the formulation [17]. This sets $k = 0$ in (6), thus requiring only one initial condition $\mathbf{h}(t_0) = \mathbf{h}_0$ for ensuring the uniqueness of solution. In case $\alpha > 1$, $\lceil \alpha \rceil$ initial conditions are necessary. Furthermore, a FDE solver is used to solve the IVP with initial condition $\mathbf{h}(t_0) = \mathbf{h}_0$ in time interval $[t_0, t_f]$:

$$\mathbf{h}(t) = PCSolve(\alpha, \mathbf{f}_\theta, \mathbf{h}_0, [t_0, t_f]). \quad (8)$$

The name *PCSolve* comes from the fact that we use a Predictor-Corrector approach to solve the FDE numerically [17].

The predictions of the Neural ODE are then given by (8), with $\mathbf{h}_t = \hat{\mathbf{y}}_t$. Note, however, that in certain scenarios, this may not be the case and an additional NN might be employed to transform the solver output into the desired form.

In summary, the Neural FDE is composed of three main components, as shown in Figure 1:

- A NN that adjusts the FDE dynamics, \mathbf{f}_θ : the NN is a function approximator that learns a function that maps the current state of the system \mathbf{h}_t to its derivative, $\mathbf{f}(\mathbf{h}(t), t) = {}^C_0D_t^\alpha \mathbf{h}(t)$, see (6). Any arbitrary NN architecture can be used, from the simpler multi-layer perceptron to the more complex residual network (ResNet). \mathbf{f}_θ receives the data of the system being modelled as input and outputs the *results* to be used by the FDE solver (Equation (8)) to update the state of the system;
- A NN that adjusts the order of the derivative, α_ϕ : the goal of this NN is to adjust the value of $\alpha \in (0, 1)$ in Equation (7). α_ϕ receives a *previous/ initial* α value, so the value of α must be initialised. Similar to \mathbf{f}_θ , the choice of architecture for this NN is flexible. However, given that the objective is to adjust a single value, a straightforward multi-layer perceptron suffices. It is important to note that, since $\alpha \in (0, 1)$, it is imperative to ensure that the value generated by α_ϕ remains within this interval. An approach to achieve this is to employ a bounded activation function in the output layer. In the experiments detailed in this paper, a sigmoid activation function was used;
- A FDE numerical solver: to solve FDEs specialised mathematical techniques and numerical methods are necessary. Several numerical methods have been introduced in the literature to solve FDEs, however, during the development of the Neural FDE, we made the strategic decision to implement the Predictor-Corrector (PC) algorithm for FDEs, as outlined in [17]. We chose this algorithm for being general, making it suitable for both linear and nonlinear problems, as well as for single and multi-term equations. This choice provides us with greater flexibility in addressing a wide range of scenarios when using Neural FDEs. Note that any FDE solver can be used with Neural FDEs.

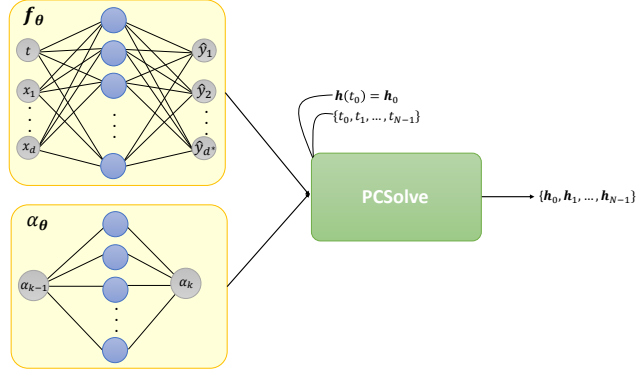


Fig. 1: Schematic of the architecture of a Neural FDE. The $PCsolve$ is used initially during model training to determine the optimal weights and biases, so that (7) fits the given data. Subsequently, the $PCsolve$ is employed again during model prediction (in this case, the NN f_{θ} and α_{ϕ} are already known, and their sole purpose is to supply the essential values required for the numerical solution of (7) to be feasible). Please refer to Algorithms (1) and (2) for a succinct explanation.

The Neural FDE comprises three components that collectively contribute to computing the loss function $\mathcal{L}_{\theta, \phi}$ during the optimisation process (training). This process aims to adjust the parameters θ, ϕ by minimising the loss function (9) (a measure of the disparity between predicted and ground truth values, such as, for example, the Mean Squared Error (MSE)); see Algorithm 1.

$$\begin{aligned} \mathcal{L}_{\theta, \phi}(\mathbf{h}(t_f)) &= \mathcal{L}_{\theta, \phi} \left(\sum_{k=0}^{\lceil \alpha \rceil - 1} \frac{t_f^k}{k!} \mathbf{h}_0^k + \frac{1}{\Gamma(\alpha)} \int_0^{t_f} (t_f - s)^{\alpha-1} f(\mathbf{h}(s), s) ds \right) \\ &= \mathcal{L}_{\theta, \phi}(PCsolve(\alpha, \mathbf{f}_{\theta}, \mathbf{h}_0, [t_0, t_f])). \end{aligned} \quad (9)$$

Given that both parameters θ and ϕ are essential for computing the predictions $\mathbf{h}(t)$, we have deduced, as a first approach, that optimising them jointly would be a good strategy. Thus, in this work, a single Adam optimiser is used to optimise the full set of parameters of the Neural FDE. Nevertheless, we recognise that there exist various possible approaches to train these parameters.

When the training of the Neural FDE has been completed, the result is a FDE, adjusted by two NNs (Figure 1). To make predictions, a numerical FDE solver is used to solve the IVP (7) and output the prediction's vector, Algorithm 2.

Algorithm 1 Neural FDE training process.

Input: start time t_0 , end time t_f , initial condition $\mathbf{h}(t_0) = \mathbf{h}_0$, maximum number of iterations $MAXITER$;
Choose *Optimiser*;
 $\mathbf{f}_\theta = DynamicsNN()$;
 $\alpha_\phi = AlphaNN()$;
Initialise θ, ϕ ;
for $k = 1 : MAXITER$ **do**
 $\alpha \leftarrow \alpha_\phi$;
 $\{\mathbf{h}_t\}_{t=t_1, t_2, \dots, t_f} \leftarrow PCSolve(\alpha, \mathbf{f}_\theta, \mathbf{h}_0, [t_0, t_f])$;
 Evaluate loss \mathcal{L} ;
 $\nabla \mathcal{L} \leftarrow$ Compute gradients of \mathcal{L} ;
 $\theta, \phi \leftarrow Optimiser.Step(\nabla \mathcal{L})$;
end for
Return: θ, α ;

Algorithm 2 Neural FDE prediction process.

Input: start time t_0 , end time t_f , initial condition $\mathbf{h}(t_0) = \mathbf{h}_0$, parameters θ , order α ;
Load \mathbf{f}_θ ;
 $\{\mathbf{h}_t\}_{t=t_1, \dots, t_f} \leftarrow PCSolve(\alpha, \mathbf{f}_\theta, \mathbf{h}_0, [t_0, t_f])$;
Return: $\{\mathbf{h}_t\}_{t=t_1, t_2, \dots, t_f}$;

The solver implemented within the Neural FDE allows the use of fixed-step solvers. As in the Neural ODE, when employing a fixed-step solver without explicitly specifying the step size Δt (default case), the time interval discretization occurs solely based on the time-steps forced by the time-series training data. However, when the step size is explicitly specified, the discretization takes place for each sub-interval (t_n, t_{n+1}) with the specified step size yielding $(t_{n+1} - t_n)/\Delta t$ time steps for each sub-interval. If the mesh points do not match the training data, an interpolation is used. This is illustrated in Figure 2.

Remark 5: It's important to note that, in most cases, solving FDEs of this nature results in a singularity at the origin. To tackle this issue, certain solvers incorporate a mesh refinement specifically in the vicinity of the origin. It's worth mentioning that, in the future, we plan to implement this graded mesh approach as a standard practice.

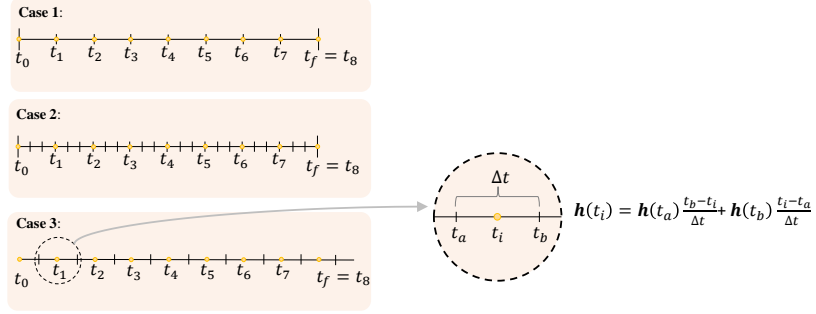


Fig. 2: Mesh refinement process employed in the solver, along with an illustration of linear interpolation. Case 1: the time mesh nodes (dash) used in the numerical method aligns with the input data series (symbols); Case 2: the time mesh used in the numerical method is now more refined, but for specific mesh nodes it aligns with the input data series; Case 3: the time mesh nodes used in the numerical method can be more refined or not, but they do not align with the input data series. The numerical solution is obtained for all mesh nodes considered, but for training purposes only the solutions at t_1, t_2, \dots are considered, being these obtained by linear interpolation (this methodology can also be used for irregularly sampled data).

Non-locality and Memory Effects

Neural FDE offer advantages over Neural ODE in modelling time-series data, primarily because of their inherent ability to capture long-term memory. When solving an FDE, the current time step t is influenced by the entire past history of the system under consideration (see Figure 3). This challenges the traditional concept of causality found in ODEs, and inherent to Neural ODEs. While ODEs typically relate a future state to its immediate preceding state, FDEs acknowledge that the current state can be influenced by all past states, emphasising a non-local and memory-dependent perspective on causality. This memory effects introduce a broader range of interactions and dependencies, leading to complex behaviours that cannot be adequately captured by ODE models.

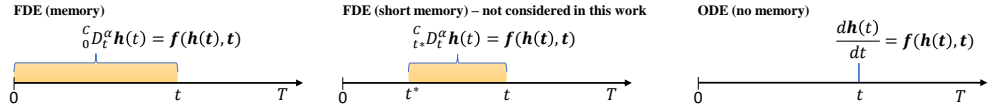


Fig. 3: Memory in FDEs (left) and ODEs (right). Schematic of the computation of the derivative (fractional or classical) at instant t . The case of short memory (center) is presented for illustrative purposes, aiming to facilitate a clear understanding of this phenomenon.

Computational Cost

The computational cost of the Neural FDE surpasses that of the Neural ODE, primarily owing to its non-local property. A significant factor contributing to the computational expenses in Neural FDE is the memory cost associated with the FDE solver. Unlike ODE solvers in Neural ODE, which rely on information from the immediate past time step, FDE solvers must retain values of the function at all preceding time steps to accurately compute subsequent ones. This storage of historical data substantially increases computational overhead [17].

The memory cost also plays a crucial role during backpropagation through the FDE solver. When training Neural FDE models, the necessity to backpropagate through all preceding time steps further amplifies the computational burden, resulting in longer training times compared to Neural ODE models.

The characteristic of Neural ODEs makes them a more efficient choice for modelling systems with simple dynamics and where memory is not a critical factor. However, while the higher computational cost may be a disadvantage, it is important to carefully consider the advantages of using Neural FDEs.

4 Numerical Experiments

To assess the performance of the architectural framework proposed in this study, a comprehensive series of experiments was carried out on a variety of datasets. First, four synthetic toy datasets were generated by numerically solving their corresponding differential equations. These datasets were specifically designed to model four distinct and well-established systems governed by differential equations: Relaxation Oscillation Process (RO), Population Growth (PG), RC Circuit Capacitor (RC), and Substance Decay (SD). For each dataset, three experiments were conducted to comprehensively evaluate the performance of the models:

- *Reconstruction*: assesses the models' capability to learn the dynamics of the training set. The evaluation is carried out using the same set for training and testing, consisting of 200 points within the time interval $t = [0, 200]$. This scenario provides insights into how well the models can reproduce the observed dynamics within the specified temporal range;
- *Extrapolation*: evaluates the performance of the models in predicting unseen time horizons to simulate a future prediction scenario. The training set encompasses 200 points in the time interval $t = [0, 200]$, while the test set includes 200 points within the extended time interval $t = [0, 300]$. This experiment represents a challenging task, examining the models' generalisation capability and the ability to extrapolate beyond the observed temporal range;
- *Completion*: evaluates the effectiveness of the models in missing data imputation, simulating a scenario where data are missing and need to be estimated. The training set comprises 200 points in the time interval $t = [0, 200]$, and the test set includes 400 points within the time interval $t = [0, 200]$.

Furthermore, four different fractional derivative orders, specifically 0.3, 0.5, 0.8, 0.99, were used to generate four FDE datasets for each system. This

selection of fractional derivative orders was made to systematically examine the capabilities and limitations of the Neural FDE in diverse scenarios. In addition, one ODE dataset was also generated to evaluate the performance of Neural FDE in modelling ODE generated data. The Neural ODE was used as a baseline in all experiments and its performance was also tested using the ODE’s and FDE’s datasets.

To accommodate the randomness of the optimisation process, three independent runs were conducted for each architecture. Model assessment relied on the average Mean Squared Error (MSE_{avg}) and its standard deviation (std).

In all experiments we used the same architecture f_{θ} for the Neural ODE and Neural FDE with: an input layer with a neuron and hyperbolic tangent (tanh) activation function; 2 hidden layers with 64 neurons and tanh activation function; and an output layer with a neuron. Since the Neural FDE has another NN, α_{ϕ} , we use a one neuron input layer with tanh activation function, a hidden layer with 32 neurons with tanh activation function, and an output layer with a neuron and a sigmoid activation function. We always initialise the α value at 0.99, in the iterative procedure.

All implementations were done in *Pytorch* and the Neural ODE was used through *Torchdiffeq* [11]. FDE solvers, namely PECE (herein designated PC) [17] were intentionally developed for this work. These solvers were adapted to ensure compatibility with NNs and backpropagation through *autograd*, and they are CUDA-enabled for efficient GPU utilisation. This tailored implementation allows for the seamless integration of FDE solvers into the PyTorch framework. Additionally, the implementation of the PC solver can be used solely for solving FDEs without using NNs and with CUDA acceleration. To the best of our knowledge, this is the first publicly available implementation of the PC solver for FDEs in *Pytorch* and being CUDA-enabled.

The numerical experiments for the RC and SD systems can be found in Appendix B.1 and Appendix B.2, respectively.

All computations were performed in a Google Cloud machine type g2-standard-32 with an Intel Cascade Lake 32 vCPU, 128GB RAM and a NVIDIA L4 GPU. The implementations can be found at [LINK]¹.

Remark 6: Please note that the main purpose of this section is not to establish superiority between the different neural network architectures. Each architecture has its own distinct advantages and disadvantages, which depend on the dynamics of the system. Overall, we will see that the Neural FDE outperforms the Neural ODE, but it’s important to recognise that the mesh refinement employed during training and testing significantly impacts the final results, making a fully equitable comparison challenging (see Appendix A for more details). Consequently, the results presented here should be viewed as a parametric examination of the behaviour of both Neural ODEs and Neural FDEs using various datasets. This serves as a means to assess and explore the methodologies outlined in the preceding sections.

4.1 Relaxation Oscillation Process

Relaxation oscillations are a phenomenon observed in various natural and engineered systems, where the dynamics alternate between periods of slow relaxation and rapid

¹available after acceptance

oscillations. Consider a system governed by the fractional-order relaxation oscillation equation:

$${}_0^C D_t^\alpha x(t) + x(t) = 1, \quad x(0) = x_0,$$

where ${}_0^C D_t^\alpha$ represents a fractional derivative operator of order α and $x(t)$ represents the variable that undergoes relaxation oscillations. The initial condition x_0 sets the initial value of x at $t = 0$, determining the starting point of the oscillatory behaviour (we consider $x(t_0) = 0.3$). In this fractional-order relaxation oscillation process, the variable $x(t)$ evolves over time. The system’s behaviour alternates between periods of slow relaxation and rapid oscillation as it approaches the equilibrium solution $x(t) = 1$.

Considering the well known limitations in the convergence of the numerical method [17] for highly singular solutions, in this first case study we focused solely on datasets corresponding to fractional-order values of $\alpha = 0.8, 0.99$, and 1 (ODE). This means that the differences between the different datasets may be smaller when compared to the case studies presented in the future subsections.

The results are organised in Table 1 and Table 2 for the Neural ODE and the Neural FDE, respectively. Additionally, the learnt α values by the Neural FDE, for the three runs, are presented in Table 3. The datasets $P_{\alpha=0.8}$, $P_{\alpha=0.99}$, and P_{ODE} are constructed with their respective α values. For P_{ODE} , α is set to 1.

Table 1: Performance of Neural ODE when modelling the RO regularly-sampled system ($MSE_{avg} \pm \text{std}$).

DATASET	RECONSTRUCTION	EXTRAPOLATION	COMPLETION
$P_{\alpha=0.8}$	$2.69\text{E-}2 \pm 3.63\text{E-}2$	$6.40\text{E-}2 \pm 6.42\text{E-}2$	$2.51\text{E-}2 \pm 3.42\text{E-}2$
$P_{\alpha=0.99}$	$9.52\text{E-}2 \pm 1.05\text{E-}1$	$8.40\text{E-}2 \pm 9.50\text{E-}2$	$1.13\text{E-}1 \pm 1.19\text{E-}1$
P_{ODE}	$3.47\text{E-}1 \pm 3.65\text{E-}1$	$3.50\text{E-}1 \pm 3.68\text{E-}1$	$3.47\text{E-}1 \pm 3.65\text{E-}1$

Table 2: Performance of Neural FDE when modelling the RO regularly-sampled system ($MSE_{avg} \pm \text{std}$).

DATASET	RECONSTRUCTION	EXTRAPOLATION	COMPLETION
$P_{\alpha=0.8}$	$3.72\text{E-}4 \pm 1.31\text{E-}4$	$1.43\text{E-}2 \pm 6.32\text{E-}4$	$3.85\text{E-}4 \pm 1.26\text{E-}4$
$P_{\alpha=0.99}$	$3.95\text{E-}4 \pm 1.44\text{E-}5$	$6.36\text{E-}4 \pm 6.14\text{E-}5$	$1.12\text{E-}3 \pm 3.64\text{E-}5$
P_{ODE}	$8.80\text{E-}5 \pm 1.47\text{E-}5$	$2.36\text{E-}4 \pm 1.10\text{E-}4$	$1.06\text{E-}4 \pm 2.90\text{E-}5$

Table 1 and Table 2 illustrate that the proposed Neural FDE exhibits significantly superior performance, for all datasets, compared to Neural ODE, with MSE_{avg} being lower by at least two orders of magnitude. It is noteworthy that Neural FDE achieved a reduction of at least three orders of magnitude in error when fitting to the dataset generated by the ODE, in contrast to Neural ODE. This evidences the performance improvement over Neural ODEs. Although, it should be mentioned that this results were obtained with no mesh refinement in both training and testing. This justifies the fact that the Neural ODE is presenting a higher error when predicting results with a model trained with its *own dataset*, P_{ODE} . For a more refined mesh, we would expect

for the Neural ODE to perform better than the Neural FDE, when considering the dataset P_{ODE} (see Appendix A). The disparity in the errors obtained will be reduced in the upcoming case studies.

Moreover, Figure 4 highlights the notably faster convergence speed of Neural FDEs compared to Neural ODEs, underscoring the superiority of our proposed Neural FDE as the preferred choice. It is important to note that the 200 iterations mentioned are unrelated to the 200 data points used in constructing some datasets.

Table 3: Adjusted α at each run for each dataset of the RO system.

	$\alpha = 0.8$	$\alpha = 0.99$	ODE
1	0.3885	0.3451	0.3015
2	0.5477	0.3923	0.4431
3	0.4472	0.4684	0.3692

The α values learnt by the Neural FDE, Table 3, show no significant patterns beyond staying relatively low, *i.e.* lower than 0.5. The expected outcome was to achieve α values closer to those used in the training set. The observed lower values can be attributed to inadequate mesh refinement, too few training iterations, and the potential minimal impact of the α_ϕ NN on the loss function (something that should be addressed in the future).

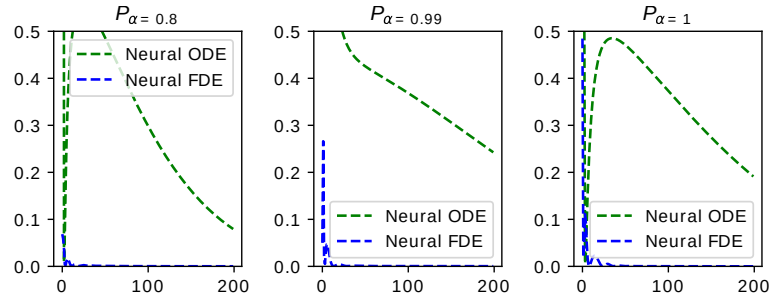


Fig. 4: Evolution of the loss during training for the three datasets $P_\alpha = 0.8, 0.99, 1$ of the RO system (loss vs. iterations).

4.2 Population Growth

Consider a population of organisms that follows a fractional-order logistic growth. The population size $P(t)$ at time t is governed by the following fractional-order differential equation:

$${}_0^C D_t^\alpha P(t) = rP(t) \left(1 - \frac{P(t)}{K} \right), \quad P(t_0) = 100,$$

where ${}_0^C D_t^\alpha$ represents the fractional derivative of order α , $r = 0.1$ is the growth rate, and $K = 1000$ is the carrying capacity of the environment. Consider the initial condition $P(t_0) = 100$. Please note that when employing fractional derivatives, the model parameters no longer have classical dimensions, as is the case when $\alpha = 1$. These modified parameters are commonly referred to as *quasiproperties*.

This equation encapsulates the intricate dynamics of the population’s growth, incorporating both fractional-order derivatives and the logistic growth model. The term $rP(t) \left(1 - \frac{P(t)}{K}\right)$ characterises the population’s net reproduction rate as a function of its current size relative to the environment’s carrying capacity. The fractional derivative $D_t^\alpha P(t)$ introduces a nuanced temporal aspect, accounting for non-integer-order rates of change in population size over time.

The results are organised in Table 4 and Table 5 for the Neural ODE and the Neural FDE, respectively. Additionally, the learnt α values by the Neural FDE, for the three runs, are shown in Table 6. To analyse and compare the convergence of Neural ODE and Neural FDE, the loss values during training were plotted in Figure 5.

Table 4: Performance of Neural ODE when modelling the PG regularly-sampled system ($MSE_{avg} \pm \text{std}$).

DATASET	RECONSTRUCTION	EXTRAPOLATION	COMPLETION
$P_{\alpha=0.3}$	7.70E-3 \pm 2.15E-5	1.04E-2 \pm 1.54E-5	7.67E-3 \pm 2.15E-5
$P_{\alpha=0.4}$	3.90E-2 \pm 2.45E-2	4.17E-2 \pm 1.91E-2	3.90E-2 \pm 2.45E-2
$P_{\alpha=0.5}$	4.91E-2 \pm 6.26E-3	5.57E-2 \pm 5.85E-3	4.92E-2 \pm 6.23E-3
$P_{\alpha=0.8}$	6.95E-2 \pm 7.11E-3	6.74E-2 \pm 1.37E-2	6.94E-2 \pm 7.19E-3
$P_{\alpha=0.99}$	4.58E-2 \pm 1.50E-3	3.45E-2 \pm 4.44E-4	4.58E-2 \pm 1.50E-3
P_{ODE}	8.33E-2 \pm 5.19E-2	7.91E-2 \pm 6.29E-2	8.34E-2 \pm 5.19E-2

Table 5: Performance of Neural FDE when modelling the PG regularly-sampled system ($MSE_{avg} \pm \text{std}$).

DATASET	RECONSTRUCTION	EXTRAPOLATION	COMPLETION
$P_{\alpha=0.3}$	1.58E-3 \pm 7.34E-4	2.97E-3 \pm 9.06E-4	1.96E-3 \pm 7.33E-4
$P_{\alpha=0.4}$	4.03E-3 \pm 7.78E-4	7.36E-3 \pm 1.25E-3	5.01E-3 \pm 6.51E-4
$P_{\alpha=0.5}$	1.99E-2 \pm 1.29E-3	2.45E-2 \pm 1.61E-3	2.06E-2 \pm 1.30E-3
$P_{\alpha=0.8}$	1.69E-2 \pm 9.29E-3	1.62E-2 \pm 4.83E-3	1.77E-2 \pm 9.55E-3
$P_{\alpha=0.99}$	1.32E-2 \pm 2.05E-3	8.97E-3 \pm 9.89E-4	1.45E-2 \pm 1.91E-3
P_{ODE}	1.15E-2 \pm 1.49E-3	7.84E-3 \pm 9.49E-4	1.30E-2 \pm 1.37E-3

Table 4 and Table 5 illustrate that the performance of both the Neural ODE and the Neural FDE is comparable in the tasks of reconstruction and completion. However, Neural FDE outperforms Neural ODE in the extrapolation task, exhibiting a lower MSE_{avg} , being similar for $P_{\alpha=0.5}$ and $P_{\alpha=0.8}$. This superiority underscores the significance of the memory mechanism employed by Neural FDEs, which allows models to leverage the entire historical context of the time series for making predictions. Furthermore, this memory scheme empowers Neural FDEs to capture more

intricate relationships within the data, consequently achieving enhanced performance, particularly in challenging tasks involving predictions for unseen time horizons.

From Figure 5, it is evident that Neural FDE exhibits significantly faster convergence compared to Neural ODE, achieving lower loss values in considerably less time. This rapid convergence, coupled with its superior performance, positions Neural FDE as a highly competitive network.

Table 6: Adjusted α at each run for each dataset of the PG regularly-sampled system.

	$\alpha = 0.3$	$\alpha = 0.4$	$\alpha = 0.5$	$\alpha = 0.8$	$\alpha = 0.99$	ODE
1	0.2792	0.214	0.3582	0.4383	0.3061	0.2824
2	0.367	0.2369	0.3268	0.2581	0.306	0.2847
3	0.2849	0.2363	0.3917	0.411	0.3631	0.3374

Once again, the α values learnt by Neural FDE, Table 6, show no significant patterns beyond staying relatively low, *i.e.* lower than 0.4.

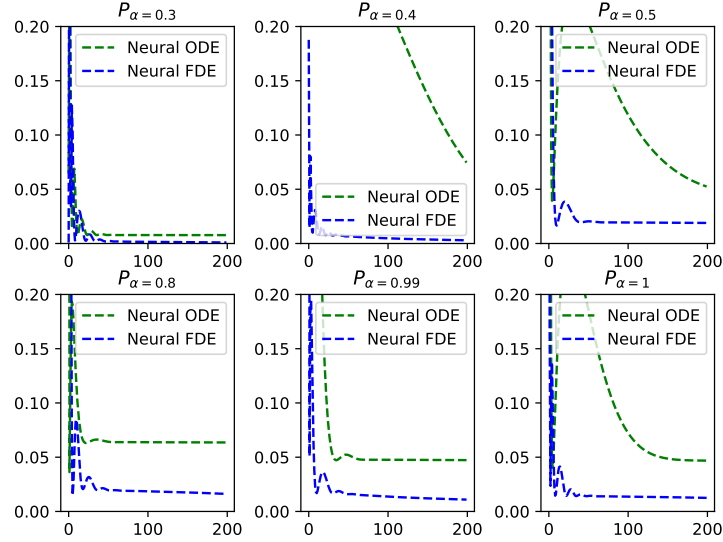


Fig. 5: Evolution of the loss during training for the four datasets of the PG system using a regularly sampled dataset (loss vs. iterations).

5 Discussion and Conclusion

Considering the concepts of Neural ODE [1] and fractional calculus in Neural systems [14], we have developed the Neural FDE to deal with time-series data. This is a FDE featuring a Caputo fractional derivative on the left-hand side (representing the

variation of the state of a dynamical system) and a *function* (\mathbf{f}_θ) of the weights and biases of a NN on the right-hand side. The goal is to accurately fit the provided data. The Neural FDE is specifically designed for dynamical systems with strong memory effects. During the Neural FDE training, we use a specialised numerical solver for FDEs to compute the solution of the pseudo FDE. Subsequently, a loss function is employed to compare the numerically predicted outcomes with the ground truth. Using *autograd* for backpropagation, we adjust the weights and biases within the Neural Network \mathbf{f}_θ to minimise errors. It is essential to note that the use of a fractional operator introduces an additional parameter, namely the order of the fractional derivative denoted as α . Consequently, apart from adjusting the weights and biases in the NN \mathbf{f}_θ , we also incorporate a separate NN to determine the optimal value for α . This implies that, during the optimisation process, adjustments are made to the weights and biases in two distinct NNs.

In the study by Chen et al. [1], the explanation regarding the numerical methods for solving differential equations was somewhat unclear. Therefore, in this work, we provide a clear explanation of how mesh refinement can be performed and how this refinement can be applied to handle irregularly sampled data.

To assess the performance of the architectural framework proposed in this study, a comprehensive series of experiments was carried out on a variety of datasets. First, four synthetic toy datasets were generated by numerically solving their corresponding differential equations. These datasets were specifically designed to model four distinct and well-established systems governed by differential equations: Relaxation Oscillation Process (RO), Population Growth (PG), RC Circuit Capacitor (RC), and Substance Decay (SD).

The experiments demonstrate that Neural FDE exhibits either significantly better or similar performance, as measured by MSE_{avg} , compared to Neural ODE. However, even in cases where the produced models demonstrate similar performance, Neural FDE showcases substantially faster convergence, achieving lower loss values in significantly fewer iterations than Neural ODE. Although, it should be mentioned that this results were obtained with no mesh refinement in both training and testing. This justifies the fact that in some cases the Neural ODE presents a higher error when predicting results with a model trained with its *own generated dataset*. For a more refined mesh, we would expect for the Neural ODE to perform better than the Neural FDE in this particular case. Note also that in some cases the computational times of the Neural FDE are prohibitive, and therefore, a mesh refinement study is provided in Appendix A for a very simple case study.

Although the Neural FDE presented in this work behaves well for the different case studies considered, there is plenty of room for improvements:

- The use of FDEs needs the computation of the entire history of the dynamical system at every time step, requiring the storage of all variables. Additionally, we employed *autograd* for backpropagation. This results in a significantly higher computational cost compared to Neural ODEs.
- When computing the loss function, we consider the weights and biases for the NN \mathbf{f}_θ , as well as weights and biases for the NN α_ϕ , optimising the order of the fractional

derivative. Our numerical results indicate that this loss function does not yield optimal orders for the fractional derivative. Therefore, in future work, we should explore a different loss function that prioritises minimising the error while also optimising the order of the fractional derivative.

- While the study by Chen et al. [1] does not explicitly address it, Neural ODEs exhibit stability issues. These problems are likewise present in Neural FDEs and stem from significant variations in weight matrices as they evolve in time. In the future, it is advisable to enhance the model’s stability by incorporating constraints within the loss function. These constraints would enable better control over the smoothness of the weight matrix evolution.
- The Predictor-Corrector numerical method, employed to solve the FDE [17], exhibits a convergence order of $\mathcal{O}(h^p)$, where h denotes the time-step and $p = \min(2, 1 + \alpha)$. In simpler terms, this implies that lower values of α can yield convergence orders of 1. It’s worth noting that the dependence of the convergence order on α is a common characteristic. To address this, one potential solution is the use of more robust numerical methods or the implementation of graded meshes, especially in the vicinity of the singularity at $t = 0$.

Acknowledgements. The authors acknowledge the funding by Fundação para a Ciência e Tecnologia (Portuguese Foundation for Science and Technology) through CMAT projects UIDB/00013/2020 and UIDP/00013/2020 and the funding by FCT and Google Cloud partnership through projects CPCA-IAC/AV/589164/2023 and CPCA-IAC/AF/589140/2023.

C. Coelho would like to thank FCT for the funding through the scholarship with reference 2021.05201.BD.

This work is also financially supported by national funds through the FCT/MCTES (PIDDAC), under the project 2022.06672.PTDC - iMAD - Improving the Modelling of Anomalous Diffusion and Viscoelasticity: solutions to industrial problems.

References

- [1] Chen, R.T., Rubanova, Y., Bettencourt, J., Duvenaud, D.K.: Neural ordinary differential equations. *Advances in neural information processing systems* **31** (2018)
- [2] Podlubny, I.: *Fractional differential equations: an introduction to fractional derivatives, fractional differential equations, to methods of their solution and some of their applications*. *Mathematics in science and engineering* **198**, 1–340 (1999)
- [3] Herrmann, R.: *Fractional Calculus: An Introduction for Physicists*, 2. ed edn. World Scientific, New Jersey, NJ (2014). <https://doi.org/10.1142/9789814551083>
- [4] Coelho, C., Costa, M.F.P., Ferrás, L.L.: Tracing footprints: Neural networks meet non-integer order differential equations for modelling systems with memory. In: *Tiny Papers @ ICLR* (2024). <https://openreview.net/forum?id=8518dcW4hc>

- [5] He, K., Zhang, X., Ren, S., Sun, J.: Deep residual learning for image recognition. In: Proceedings of the IEEE Conference on Computer Vision and Pattern Recognition (CVPR) (2016)
- [6] Haber, E., Ruthotto, L., Holtham, E., Jun, S.-H.: Learning across scales—multiscale methods for convolution neural networks. Proceedings of the AAAI Conference on Artificial Intelligence **32**(1) (2018) <https://doi.org/10.1609/aaai.v32i1.11680>
- [7] Haber, E., Ruthotto, L.: Stable architectures for deep neural networks. Inverse Problems **34**(1), 014004 (2017) <https://doi.org/10.1088/1361-6420/aa9a90>
- [8] E, W.: A proposal on machine learning via dynamical systems. Communications in Mathematics and Statistics **5**(1), 1–11 (2017) <https://doi.org/10.1007/s40304-017-0103-z>
- [9] Lu, Y., Zhong, A., Li, Q., Dong, B.: Beyond finite layer neural networks: Bridging deep architectures and numerical differential equations. In: Dy, J., Krause, A. (eds.) Proceedings of the 35th International Conference on Machine Learning. Proceedings of Machine Learning Research, vol. 80, pp. 3276–3285. PMLR, ??? (2018). <https://proceedings.mlr.press/v80/lu18d.html>
- [10] Ruthotto, L., Haber, E.: Deep neural networks motivated by partial differential equations. Journal of Mathematical Imaging and Vision **62**(3), 352–364 (2019) <https://doi.org/10.1007/s10851-019-00903-1>
- [11] Chen, R.T.Q.: torchdiffeq (2018). <https://github.com/rtqichen/torchdiffeq>
- [12] Diethelm, K.: The Analysis of Fractional Differential Equations: An Application-Oriented Exposition Using Differential Operators of Caputo Type. Springer, ??? (2010). <https://doi.org/10.1007/978-3-642-14574-2> . <http://dx.doi.org/10.1007/978-3-642-14574-2>
- [13] Liu, Y., Roberts, J., Yan, Y.: A note on finite difference methods for nonlinear fractional differential equations with non-uniform meshes. International Journal of Computer Mathematics **95**(6-7), 1151–1169 (2018) <https://doi.org/10.1080/00207160.2017.1381691>
- [14] Lundstrom, B.N., Higgs, M.H., Spain, W.J., Fairhall, A.L.: Fractional differentiation by neocortical pyramidal neurons. Nature Neuroscience **11**(11), 1335–1342 (2008) <https://doi.org/10.1038/nn.2212>
- [15] Diethelm, K., Ford, N.J.: Analysis of fractional differential equations. Journal of Mathematical Analysis and Applications **265**(2), 229–248 (2002) <https://doi.org/10.1006/jmaa.2000.7194>
- [16] Barros, L.C.d., Lopes, M.M., Pedro, F.S., Esmi, E., Santos, J.P.C.d., Sánchez,

D.E.: The memory effect on fractional calculus: an application in the spread of covid-19. *Computational and Applied Mathematics* **40**(3) (2021) <https://doi.org/10.1007/s40314-021-01456-z>

- [17] Diethelm, K., Ford, N.J., Freed, A.D.: A Predictor-Corrector Approach for the Numerical Solution of Fractional Differential Equations. *Nonlinear Dynamics* **29**(1), 3–22 (2002)
- [18] Kaslik, E., Sivasundaram, S.: Nonlinear dynamics and chaos in fractional-order neural networks. *Neural Networks* **32**, 245–256 (2012) <https://doi.org/10.1016/j.neunet.2012.02.030>

A Numerical Method and Mesh Refinement

Consider solving an ODE IVP (Equation (5)) and the FDE IVP (Equation (7)), with initial condition $\mathbf{h}(t_0) = \mathbf{h}_0$ for time-steps (t_0, t_1, \dots, t_f) . When employing a fixed-step solver, the time interval is discretized according to the time-steps provided (Algorithm 3):

Algorithm 3 Solving an ODE with a fixed-step solver.

Input: discretization time steps $t = (t_0, t_1, \dots, t_f)$, initial condition $\mathbf{h}(t_0) = \mathbf{h}_0$;
 $\{\mathbf{h}_t\}_{t=t_0, t_1, \dots, t_f} \leftarrow \text{ODESolve}(\mathbf{f}_\theta, \mathbf{h}_0, (t_0, t_1, \dots, t_f))$;
Return: $\{\mathbf{h}_t\}_{t=t_0, t_1, \dots, t_f}$;

Now, consider solving the same ODE IVP using a fixed-step solver across the time interval $[t_0, t_f]$ using a step size smaller than $t_1 - t_0$. This process involves dividing the interval into sub-intervals (t_n, t_{n+1}) with a uniform step size Δt , resulting in $N = (t_{n+1} - t_n)/\Delta t$ time steps per sub-interval. Subsequently, the solver proceeds to solve the ODE within each sub-interval (Algorithm 4). If, however, the selected step size fails to encompass the endpoint t_{n+1} , the state is computed by interpolation (see Figure 2).

Algorithm 4 Solving an ODE with a fixed-step solver with a chosen step size.

Input: time steps $t = (t_0, t_1, \dots, t_f)$, initial condition $\mathbf{h}(t_0) = \mathbf{h}_0$, step size Δt ;
for $n = 1 : f$ **do**
 $N \leftarrow \frac{t[n] - t[n-1]}{\Delta t}$;
 $\{\mathbf{h}_t\}_{t=t[n-1], t[n]} \leftarrow \text{ODESolve}(\mathbf{f}_\theta, \mathbf{h}_0, (t[n-1], t[n-1] + \Delta t, \dots, t[n-1] + \Delta t \times N))$;
end for
Return: $\{\mathbf{h}_t\}_{t=t_0, t_1, \dots, t_f}$; (linear interpolation may be needed)

The choice of the step size is of paramount importance. Smaller Δt in the discretization process using a fixed-step solver with sub-interval discretization, Algorithm 4, offers a pathway to enhancing the accuracy and reliability of the approximated solution. By decreasing Δt , each sub-interval is divided into more steps, becoming finer. This finer resolution enables the solver to capture intricate features and rapid changes in the solution that may occur within shorter time frames. Consequently, the computed solution becomes more faithful to the true behaviour of the system, especially in regions of high variability or steep gradients. Also, smaller Δt helps mitigate errors inherent to numerical methods. Thus, selecting the appropriate Δt poses a significant challenge due to the trade-off between accuracy of the solution and computational cost. Moreover, the optimal Δt may vary throughout the solution domain, complicating the task of selecting a single value that adequately balances accuracy and efficiency

across the entire computation. To remove the need for selecting an appropriate fixed step size, adaptive-step solvers were introduced (these are only available in this work for the Neural ODE). Similar to Algorithm 4, adaptive-step solvers divide t into sub-intervals however, Δt is computed and dynamically adjusted during the integration process, based on the local behaviour of the solution. This adaptability allows the solver to allocate smaller steps in regions where the solution changes rapidly or exhibits intricate features, while larger steps are used in smoother regions where the solution varies more gradually. Thus, when employing Algorithm 3, if the step size inherent to t , given by $t_1 - t_0$, is substantial then the solutions approximation may be inaccurate and most likely lack the accuracy of the approximations done with Algorithm 4 and an adaptive-step solver. Furthermore, when the step size of a fixed-step solver is sufficiently small, the approximation accuracy can reach, and in some cases exceed, that achieved by adaptive-step solvers.

To demonstrate how the choice of step size influences the fit of Neural ODEs and Neural FDEs to the system under study, we conducted some simple experiments. We used the PG system to generate four datasets, each covering a smaller time domain $t = [0, 10]$ with 50 data points. These datasets were created in two variations: two were derived by solving an ODE with step sizes of 1 and 0.1, while the other two were obtained by solving an FDE with $\alpha = 0.8$ using step sizes of 1 and 0.1. Subsequently, we employed both a Neural ODE to learn the ODE generated datasets and a Neural FDE to fit the FDE generated datasets. We then performed an analysis of the plots depicting the ground truth and predicted curves, as illustrated in Figures 6-9.

From Figures 6-9, it can be seen that smaller Δt results in a more accurate approximation of the system's behaviour. This finer granularity also improves the fitting by both the Neural ODE and Neural FDE models.

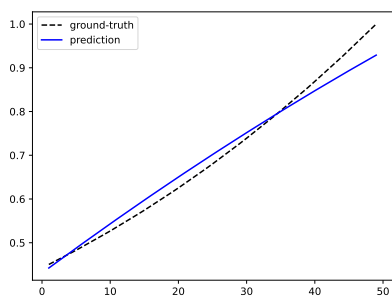


Fig. 6: ODE dataset with $\Delta t = 1$.

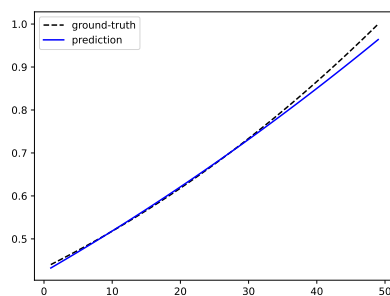


Fig. 7: ODE dataset with $\Delta t = 0.1$.

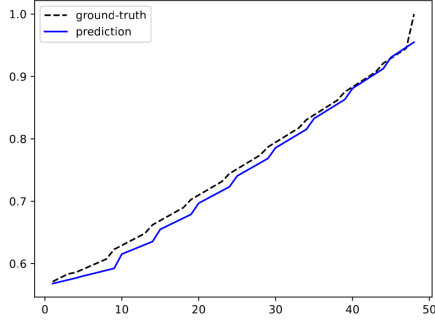


Fig. 8: FDE dataset $\alpha = 0.8$ with $\Delta t = 1$.

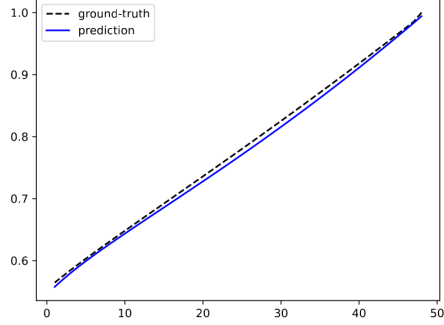


Fig. 9: FDE dataset $\alpha = 0.8$ with $\Delta t = 0.1$.

Fig. 10: Modelling PG datasets with Neural FDE.

B Additional Numerical Experiments

B.1 RC Circuit Capacitor

Consider an RC circuit with a fractional-order capacitor. The fractional-order equation describing the circuit is given by:

$${}_0^C D_t^\alpha V(t) = \frac{1}{RC} V(t), \quad V(t_0) = 10,$$

where α is the fractional order between 0 and 1, $V(t)$ is the voltage across the capacitor, $R = 100$ is the resistance, and $C = 0.2$ is the fractional capacitor. The initial condition for the voltage is $V(t_0) = 10$.

This equation captures the intricate dynamics of the circuit's behaviour, combining the effects of fractional-order elements with the fundamental principles of RC circuits. The term $\frac{1}{RC} V(t)$ represents the rate of change of voltage across the fractional-order capacitor, illustrating how the circuit responds to the interplay between resistance (R), fractional capacitance (C), and the time-dependent voltage ($V(t)$).

The results are organised in Table 7 and Table 8 for the Neural ODE and Neural FDE, respectively. Additionally, the learnt α values by Neural FDE, for the three runs, are shown in Table 9. To analyse and compare the convergence of Neural ODE and Neural FDE, the loss values during training were plotted in Figure 11.

Table 7 and Table 8 demonstrate that, overall, the Neural ODE and the Neural FDE exhibit comparable performance in modelling this system. Notably, Neural FDE displays lower MSE_{avg} values for lower derivative orders ($P_{\alpha=0.3}$, $P_{\alpha=0.4}$, and $P_{\alpha=0.5}$). However, as depicted in Figure 11, while both Neural ODE and Neural FDE yield similarly performant models, Neural FDE demonstrates faster convergence of the loss function, requiring less training time.

Again, the α values learnt by Neural FDE, Table 9, show no apparent pattern, being always lower than 0.5.

Table 7: Performance of Neural ODE when modelling the RC regularly-sampled system ($MSE_{avg} \pm \text{std}$).

DATASET	RECONSTRUCTION	EXTRAPOLATION	COMPLETION
$P_{\alpha=0.3}$	$5.84\text{E-}2 \pm 7.88\text{E-}2$	$5.64\text{E-}2 \pm 7.44\text{E-}2$	$5.85\text{E-}2 \pm 7.89\text{E-}2$
$P_{\alpha=0.4}$	$9.56\text{E-}3 \pm 1.34\text{E-}4$	$1.50\text{E-}2 \pm 1.01\text{E-}4$	$9.56\text{E-}3 \pm 1.34\text{E-}4$
$P_{\alpha=0.5}$	$2.64\text{E-}2 \pm 6.06\text{E-}5$	$4.23\text{E-}2 \pm 1.27\text{E-}4$	$2.64\text{E-}2 \pm 6.09\text{E-}5$
$P_{\alpha=0.8}$	$6.25\text{E-}2 \pm 9.16\text{E-}5$	$5.63\text{E-}2 \pm 7.09\text{E-}4$	$6.22\text{E-}2 \pm 8.63\text{E-}5$
$P_{\alpha=0.99}$	$5.35\text{E-}2 \pm 1.62\text{E-}2$	$4.86\text{E-}2 \pm 2.23\text{E-}2$	$5.33\text{E-}2 \pm 1.63\text{E-}2$
P_{ODE}	$4.11\text{E-}2 \pm 1.19\text{E-}5$	$3.14\text{E-}2 \pm 9.43\text{E-}07$	$4.08\text{E-}2 \pm 1.15\text{E-}5$

Table 8: Performance of Neural FDE when modelling the RC regularly-sampled system ($MSE_{avg} \pm \text{std}$).

DATASET	RECONSTRUCTION	EXTRAPOLATION	COMPLETION
$P_{\alpha=0.3}$	$1.04\text{E-}3 \pm 5.66\text{E-}4$	$1.70\text{E-}3 \pm 8.13\text{E-}4$	$1.21\text{E-}3 \pm 5.06\text{E-}4$
$P_{\alpha=0.4}$	$2.83\text{E-}3 \pm 1.03\text{E-}3$	$6.39\text{E-}3 \pm 1.50\text{E-}3$	$3.32\text{E-}3 \pm 1.03\text{E-}3$
$P_{\alpha=0.5}$	$8.08\text{E-}3 \pm 2.11\text{E-}3$	$2.11\text{E-}2 \pm 3.40\text{E-}3$	$9.22\text{E-}3 \pm 2.01\text{E-}3$
$P_{\alpha=0.8}$	$4.31\text{E-}2 \pm 5.17\text{E-}3$	$4.54\text{E-}2 \pm 2.41\text{E-}3$	$4.47\text{E-}2 \pm 5.19\text{E-}3$
$P_{\alpha=0.99}$	$3.77\text{E-}2 \pm 2.28\text{E-}3$	$2.97\text{E-}2 \pm 1.18\text{E-}3$	$3.79\text{E-}2 \pm 1.97\text{E-}3$
P_{ODE}	$3.35\text{E-}2 \pm 9.63\text{E-}4$	$2.73\text{E-}2 \pm 2.67\text{E-}4$	$3.42\text{E-}2 \pm 1.19\text{E-}3$

Table 9: Adjusted α at each run for each dataset of the RC regularly-sampled system.

	$\alpha = 0.3$	$\alpha = 0.4$	$\alpha = 0.5$	$\alpha = 0.8$	$\alpha = 0.99$	ODE
1	0.4298	0.2956	0.2136	0.2196	0.4585	0.2427
2	0.4741	0.3883	0.2287	0.2163	0.391	0.2511
3	0.3068	0.2229	0.3092	0.3802	0.3226	0.3397

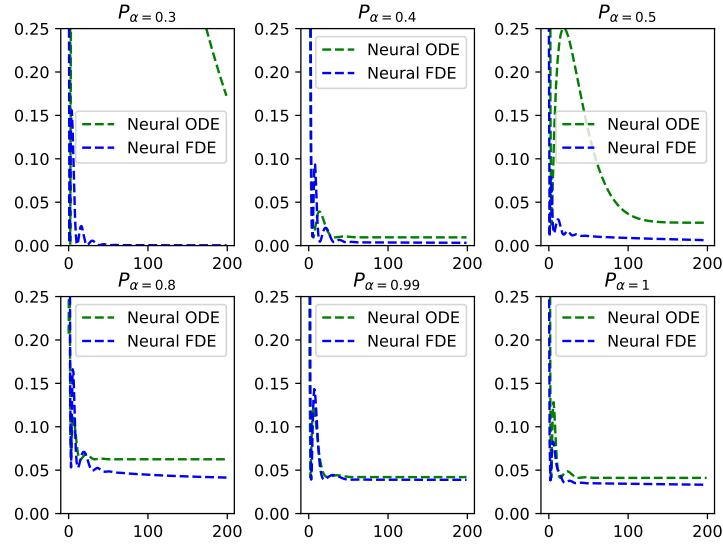


Fig. 11: Evolution of the loss during training for the four datasets of the RC system (loss vs. iterations).

B.2 Substance Decay

Consider a substance undergoing fractional-order decay with the following equation:

$${}_0^C D_t^\alpha N(t) = -\lambda N(t), \quad N(t_0) = 100,$$

where $\alpha \in (0, 1)$ represents the fractional order, $N(t)$ denotes the quantity of the decaying substance, and $\lambda = 0.5$ is the decay constant. The initial condition is $N(t_0) = 100$.

This equation captures the intricate dynamics of substance decay, incorporating both fractional-order derivatives and exponential decay principles. The term $-\lambda N(t)$ signifies the decay rate proportional to the current quantity of the substance. The fractional derivative ${}_0^C D_t^\alpha$ introduces a nuanced temporal aspect, considering non-integer-order rates of decay over time.

Interpreting and studying this fractional-order decay model could provide valuable insights into the behaviour of decaying substances, potentially offering more accurate predictions and informed decay management strategies.

The results are organised in Table 10 and Table 11 for the Neural ODE and the Neural FDE, respectively. Additionally, the learnt α values by Neural FDE, for the three runs, are shown in Table 12. To analyse and compare the convergence of the Neural ODE and the Neural FDE, the loss values during training were plotted, Figure 12.

Table 10: Performance of Neural ODE when modelling the SD regularly-sampled system ($MSE_{avg} \pm \text{std}$).

DATASET	RECONSTRUCTION	EXTRAPOLATION	COMPLETION
$P_{\alpha=0.3}$	1.43E-2 \pm 6.40E-3	3.59E-2 \pm 6.66E-3	2.86E-2 \pm 1.17E-2
$P_{\alpha=0.4}$	3.01E-2 \pm 2.84E-2	7.35E-2 \pm 6.32E-2	2.42E-2 \pm 1.02E-2
$P_{\alpha=0.5}$	1.83E-2 \pm 5.68E-3	2.32E-2 \pm 8.19E-3	1.48E-2 \pm 2.38E-3
$P_{\alpha=0.8}$	2.00E-3 \pm 2.00E-4	2.57E-3 \pm 1.95E-4	1.47E-3 \pm 1.67E-4
$P_{\alpha=0.99}$	9.17E-3 \pm 1.24E-2	9.47E-3 \pm 1.25E-2	9.06E-3 \pm 1.24E-2
P_{ODE}	6.53E-3 \pm 8.24E-3	6.55E-3 \pm 8.29E-3	6.53E-3 \pm 8.24E-3

Table 11: Performance of Neural ODE when modelling the SD regularly-sampled system ($MSE_{avg} \pm \text{std}$).

DATASET	RECONSTRUCTION	EXTRAPOLATION	COMPLETION
$P_{\alpha=0.3}$	8.78E-4 \pm 4.10E-4	4.73E-2 \pm 2.73E-3	4.55E-3 \pm 2.94E-4
$P_{\alpha=0.4}$	2.17E-3 \pm 2.01E-3	3.44E-2 \pm 5.25E-3	7.90E-3 \pm 1.75E-3
$P_{\alpha=0.5}$	1.47E-3 \pm 4.56E-4	3.77E-3 \pm 3.22E-4	1.42E-3 \pm 1.54E-4
$P_{\alpha=0.8}$	3.35E-3 \pm 3.27E-3	4.21E-3 \pm 3.88E-3	2.66E-3 \pm 2.77E-3
$P_{\alpha=0.99}$	8.07E-3 \pm 4.96E-3	9.00E-3 \pm 5.16E-3	7.06E-3 \pm 4.77E-3
P_{ODE}	1.35E-3 \pm 5.95E-4	1.86E-3 \pm 6.62E-4	9.62E-4 \pm 4.75E-4

Table 10 and Table 11 indicate that at the reconstruction task, Neural FDE exhibits superior performance for datasets generated with FDEs with $\alpha \leq 0.5$, while showing

similar performance for others. Overall, Neural FDE also demonstrates better performance at the completion task compared to Neural ODE. Both Neural ODE and Neural FDE demonstrate similar performance in extrapolation. Although the performance of Neural FDE in modelling this system may not show a substantial improvement in terms of MSE_{avg} , Figure 12 reveals that once again, the convergence rate of Neural FDE is significantly higher, leading to the need of fewer iterations when compared to Neural ODE, while achieving comparable performance.

Table 12: Adjusted α at each run for each dataset of the SD regularly-sampled system.

	$\alpha = 0.3$	$\alpha = 0.4$	$\alpha = 0.5$	$\alpha = 0.8$	$\alpha = 0.99$	ODE
1	0.2535	0.4945	0.4228	0.6092	0.4132	0.759
2	0.3598	0.508	0.3512	0.4379	0.5958	0.7184
3	0.4019	0.435	0.3446	0.6627	0.5444	0.6529

Unlike for the other systems, the α values learned by Neural FDE are generally higher, but no discernible pattern emerges, as shown in Table 12. As said before, the potential minimal impact of the α_ϕ NN on the loss function may be influencing the final α values obtained.

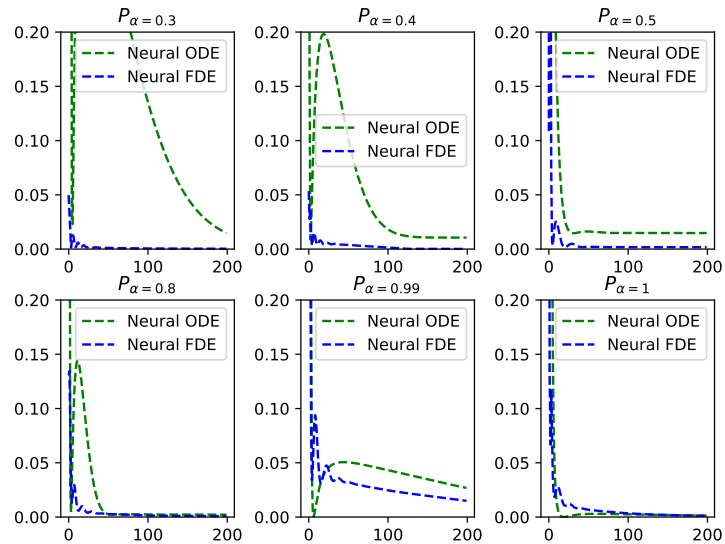


Fig. 12: Evolution of the loss during training for the four datasets of the SD system (loss vs. iterations).